

Evidence for Anomalous Effects on the Current Evolution in Tokamak Operating Scenarios

T.A. Casper 1), R.J. Jayakumar 1), S.L. Allen 1), C.T. Holcomb 1), M.A. Makowski 1), L.D. Pearlstein 1), H.L. Berk 2), C.M. Greenfield 3), T.C. Luce 3), C.C. Petty 3), P.A. Politzer 3), M.R. Wade 3), M. Murakami 4), and C.E. Kessel 5)

1) Lawrence Livermore National Laboratory, P.O. Box 808, Livermore, CA 94550, USA

2) Institute for Fusion Studies, The University of Texas, Austin, Texas, USA

3) General Atomics, P.O. Box 85608, San Diego, California 92186-5608, USA

4) Oak Ridge National Laboratory, Oak Ridge, Tennessee, USA

5) Princeton Plasma Physics Laboratory, Princeton, New Jersey, USA

e-mail contact of main author: casper1@llnl.gov

Abstract. Alternatives to the usual picture of advanced tokamak (AT) discharges are those that form when anomalous effects alter the plasma current and pressure profiles and those that achieve stationary characteristics through mechanisms so that a measure of desired AT features is maintained without external current-profile control. Regimes exhibiting these characteristics are those where the safety factor (q) evolves to a stationary profile with the on-axis and minimum $q \sim 1$ and those with a deeply hollow current channel and high values of q . Operating scenarios with high fusion performance at low current and where the inductively driven current density achieves a stationary configuration with either small or non-existing sawteeth may enhance the neutron fluence per pulse on ITER and future burning plasmas. Hollow current profile discharges exhibit high confinement and a strong “box-like” internal transport barrier (ITB). We present results providing evidence for current profile formation and evolution exhibiting features consistent with anomalous effects or with self-organizing mechanisms. Determination of the underlying physical processes leading to these anomalous effects is important for scaling of current experiments for application in future burning plasmas.

1. Introduction

Experiments worldwide have discovered inductively driven operating configurations with moderately high performance where the stationary q -profile remains at or above unity. As is evidenced by the non-time-varying pitch-angle data from motional Stark effect (MSE) measurements, these stationary conditions have been observed on several experiments in two distinctly different operating regimes, the hybrid [1,2] and quiescent double barrier (QDB) [3] modes. We address hybrid conditions here and present evidence that anomalous current diffusion can alter the q -profile evolution in DIII-D. We use modeling of discharges to compare and contrast with experimental observations.

In hybrid scenarios, while the usual feedback control of density and power are employed, a key ingredient is the ability to passively sustain a stationary current density profile with safety factor at the magnetic axis, q_0 , close to and slightly above unity and, therefore, with minimal or no sawteeth over several current diffusion times. This permits operation with higher performance and normalized β [$\beta_N = \beta/(I/aB_T)$] closer to the no-wall limit. This stationarity appears to be closely linked to the presence of continuous $n = 2$ or $n = 3$ NTM mode activity. We compare the anomalous evolution of these hybrid discharges with a modeled evolution to assess these effects. Experimental and theoretical efforts are underway to find the precise mechanism by which these NTMs or other modes interact to maintain $q_0 \sim 1$ [4].

High-confinement “current-hole” plasmas have also been generated and sustained in the DIII-D tokamak. In such discharges, the current profile is determined by a combination of the slowing down of the inductively driven flux diffusion, formation of an internal transport

barrier, and the resulting strong bootstrap current in the middle of the plasma. In a self-organizing manner, the strongly reversed shear also causes strong diffusion of fast-ions thus suppressing the usual neutral beam current drive in the core while enhancing the current drive outside the barrier. Equilibrium fits for these strongly hollow current profiles are difficult to obtain due to fast-ion redistribution in these plasmas. However, we have obtained robust MSE-constrained equilibrium fits for DIII-D current-hole discharges. We compare the kinetic fits obtained using different models for the neutral beam dynamics. We show profiles of these current components obtained from the TRANSP code that are consistent with the current and pressure profiles obtained from the experimental data.

2. Hyper-resistive Model for Current Diffusion due to NTMs in the CORSICA Code

In the CORSICA transport code [5], we have modified our Ohm's law implementation with the addition of a new hyper-resistive (current diffusion) term [6] to simulate the effects of neoclassical islands using a model by Berk, Fowler, LoDestro and Pearlstein (BFLP) [7]. This will be used in combination with an existing hyper-resistive model due to Ward and Jardin (WJ) [8]. This island physics is a relatively new addition and we outline its implementation here. The hyper-resistive effects are generated by time-independent, field-line entanglement according to the Rechester-Rosenbluth [9] approach. The additional feature is a hyper-resistive response due to the turbulence. We start with the drift-kinetic equation for electrons and perform a quasi-linear analysis [7] to obtain:

$$\frac{\partial f_0}{\partial t} + v_{\parallel} \frac{\partial f_0}{\partial s} = C(f_0) - \frac{v_{\parallel}}{B} \nabla \cdot \left(\tilde{B} |\tilde{B} \cdot \nabla \psi| \frac{v_{\parallel}}{B} \cdot \frac{\tilde{v}}{\tilde{v}^2 + k_{\parallel}^2 v_{th}^2} \frac{\partial f_0}{\partial \psi} \right) \equiv C(f_0) + D(f_0) \quad . \quad (1)$$

The first term on the right-hand side is the usual Fokker-Planck operator (C) while the second term (D) represents Rechester-Rosenbluth transport where ψ is the poloidal flux and \tilde{v} is the effective collision frequency. Ohm's law can be written as:

$$E + \frac{v}{c} \times B = \frac{m}{ne} \int v_{\parallel} d^3 v [C(f_0) + D(f_0)] \quad , \quad (2)$$

and, with the standard averages we obtain Ohm's law,

$$\begin{aligned} \frac{\partial \psi}{\partial t} &= \eta \langle J \cdot B \rangle \text{ or, with } \langle \dots \rangle = \oint \frac{dl}{B} \dots \Big/ \oint \frac{dl}{B} \quad , \\ \frac{\langle B \cdot E \rangle}{\langle B \cdot \nabla \varphi \rangle} &= \frac{\partial \psi}{\partial t} = \eta \frac{\langle J \cdot B \rangle}{\langle B \cdot \nabla \varphi \rangle} - \frac{1}{2\pi q} \frac{\partial}{\partial \psi} \oint \frac{dl}{B} \frac{m}{ne^2} |\tilde{B} \cdot \nabla \psi|^2 \left\langle \frac{\tilde{v} v_{th}^2}{\tilde{v}^2 + (k_{\parallel} v_{th})^2} \right\rangle \frac{\partial}{\partial \psi} \frac{J_{\parallel}}{B} \quad . \quad (3) \end{aligned}$$

Note that we have taken liberties by moving terms through the operators to preserve helicity conservation. The first term on the right-hand side is the usual flux diffusion term and the new term is the current diffusion. When averaging is performed, it is assumed that these terms are functions of density, n , and temperature, T . We assume that n is constant over an island.

All that remains is to determine the value of $\tilde{B} \sim w^2$ for w the island width. For this, we turn to: $\partial w / \partial t = 1.22 \eta / \mu_0 [\Delta' + (D_R / w) + D_{neo} w / (w^2 + \bar{w}^2)]$, the modified Rutherford equation [10,11] where Δ' is the cylindrical tearing mode criteria, D_R the resistive interchange term [12] and D_{neo} the neoclassical island drive. We do not include the polarization threshold term. Our purpose is to evaluate the impact of hyper-resistivity on the current and q -profile evolution. In principle, this theory contains no adjustable parameters. In practice, we can

adjust the neoclassical drive of order unity to keep the island size representative of that observed in the experiment. The use of cylindrical approximations in the theory with application to shaped tokamaks like DIII-D are likely to lead to uncertainties of this order.

3. Hyper-resistive Modeling of Hybrid Mode Current Profile Evolution

Using hyper-resistive models in the CORSICA transport code, we explore the extent to which the observed current profile evolution is consistent with modifications due to the presence of fluctuations driving diffusion of the local current density. We concentrate on a representative DIII-D hybrid mode discharge, shot 117755, with parameters shown in Fig. 1 at a toroidal field of $B_T = 1.7$ T, $\beta_N = 2.7$ and confinement factor $H_{I89} = 2.5$. Some characteristics of this discharge were previously explored [13] using an ad-hoc conductivity-flattening model to demonstrate the possibility of dynamo-like behavior. Here, we expand on these simulations with a combination of hyper-resistive models active over different regions. In these simulations using the BFLP model, we turn on a particular island based on experimental observations, Fig. 1(d). The island location, width and stability are determined from the modified Rutherford island evolution equation. These define a spatially spread hyper-resistive coefficient that alters the current density and q -profiles near the island location through Ohm's law as the equilibrium evolves. We note that this current diffusion in the simulations is present in addition to the normal flux diffusion associated with peaking of the Ohmic current near the magnetic axis. In these simulations, we use the measured electron and impurity density and electron and ion temperature profiles. The non-inductive current drive sources also simulated are the bootstrap current density (J_{BS}) from NCLASS [14] and the neutral-beam current (J_{NB}) using a Monte Carlo deposition model with a model for the ion orbits [15]. The total current (J_T) and Ohmic current (J_{OH}) densities are determined from the competition between current and flux diffusion to determine the q -profile with examples of these shown in Fig. 2 at 2.5 s during the time q is decreasing. We also show the normalized hyper-resistive coefficient resulting from the BFLP/NTM model to indicate regions where hyper-resistivity is active. Hyper-resistivity is continuously active and its cumulative effect is to alter the evolution of the q -profile.

In Fig. 3, we show simulation q -profile contours modified by hyper-resistivity and the predicted island evolution for shot 117755. The jump in the island parameters at 2.3 s is the time

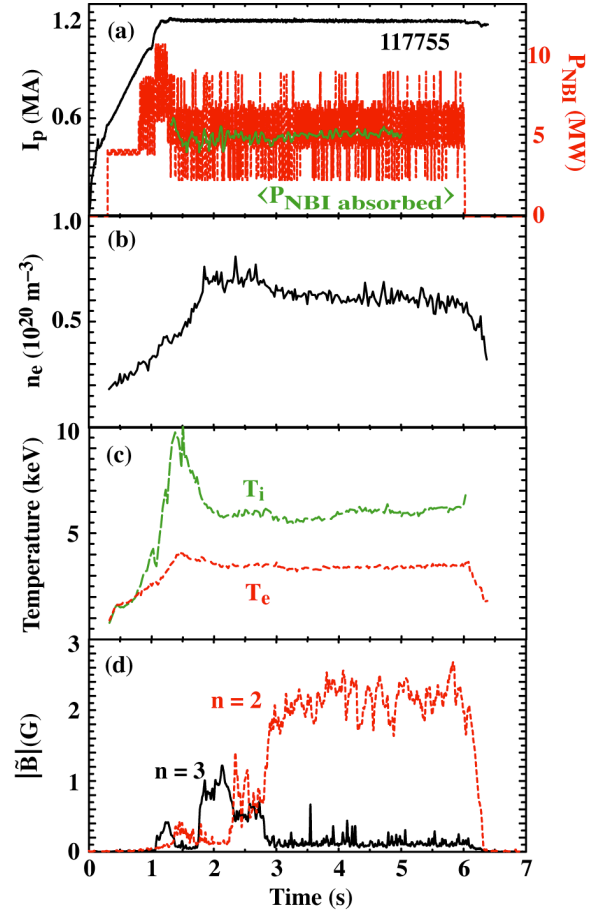


FIG. 1. DIII-D hybrid shot 117755: (a) plasma current, neutral-beam power under β_n -feedback control and average absorbed power computed in Corsica, (b) electron density, (c) electron and ion temperatures and (d) edge $n = 2, 3$ fluctuation amplitudes.

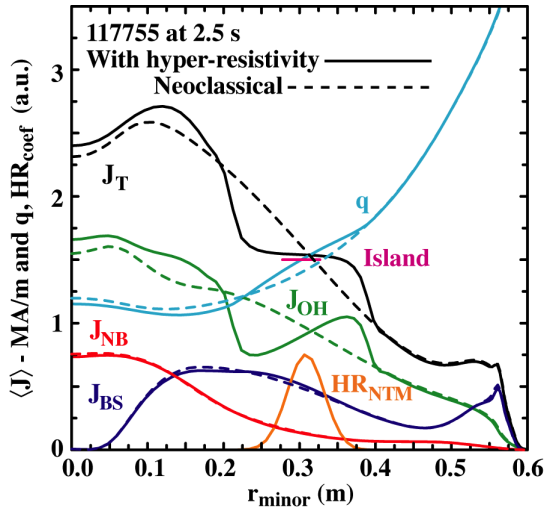


FIG. 2. Flux-averaged current densities $\langle J \rangle$, q , and normalized hyper-resistive coefficient (HR) at 2.5 s showing current diffusion due to the BFLP model flattening the J_T profile at the island and modifying the q profile evolution as compared with the neoclassical simulation.

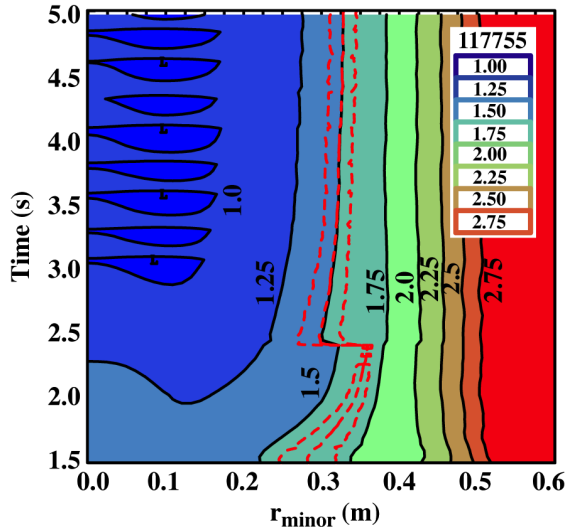


FIG. 3. Evolution of q -profile contours computed using the hyper-resistive models for 117755. The NTM island (red dashed) evolution: $R_{\text{island}} \pm W_{\text{island}}/2$. A (5,3)-mode is active from 1.55 to 2.3 s when we switched to a (3,2)-mode. The structure inside $r_{\text{minor}} = 0.15$ m is due to the WJ hyper-resistive model transiently adjusting q_0 late in time.

island location and size. Alternatively, we have included only the diamagnetic term in the radial electric field contribution to the synthetic MSE data whereas there can be a sizeable perturbation in the measurements due to toroidal rotation. At large radii (outside the island location) where the “radial” and “edge” arrays view the plasma, the agreement between simulated and real data is not as good as in the core. The radial MSE array suffers from a lack of radial resolution and we hypothesize that this is the difference between the simulated and

where we switch from (m,n) -mode number of (5,3) to a (3,2)-mode in the simulations. This change is motivated by the shift in dominant mode numbers as indicated in Fig. 1(d). The island size grows initially but saturates in width as decreasing $\Delta' < 0$ is stabilizing with respect to the neoclassical contribution. We show in Fig. 4, a comparison of the simulated temporal evolution of q_0 and q_{min} , the minimum q , obtained in CORSICA simulations with and without hyper-resistivity with those from a sequence of MSE-constrained EFIT solutions. We note the quantitatively good agreement of the simulated evolution using these hyper-resistive models with the experimentally fitted q_0 and q_{min} as compared with the neoclassical evolution. In Fig. 5(a), we show a comparison between the MSE pitch angle measurements [16] and those from a synthetic MSE diagnostic inside CORSICA [17] for a channel near the magnetic axis. This shows good time-dependent agreement between the simulated and directly measured pitch angle data indicating that the simulated evolution is in substantial agreement with the experimental observations. In the interval from 2.3 to 2.8 s the discrepancy can be slightly larger. During this time interval the $n=2$ and $n=3$ fluctuations are comparable in magnitude [Fig. 1(d)] while we have simulated only the effects of a single island. In Fig. 5(b), we also show a comparison between the profiles of the synthetic diagnostic and the MSE data averaged over the beam-on time intervals at $t = 2$ s. We find the agreement to be quite respectable, particularly towards the inside, e.g., $R < 2$ m. The discrepancy in the region of the NTM island may indicate that details of its affect on current diffusion may be slightly different than that predicted by the hyper-resistive model using a single predicted

real data. In the edge, the discrepancy is likely due to the experimental profile fits and/or the edge radial electric field but this is outside the island hyper-resistive region. In this region, the current profile includes the local peak in the bootstrap current due to the pedestal gradients. In comparisons with the lithium ion beam measurements [18], we have found better agreement between the synthetic diagnostic and the measured edge magnetic field in other H-mode discharge comparisons.

We conclude that, during the time q is decreasing and the q -profile is relaxing to a stationary state, the predictions of an anomalous current diffusion using the hyper-resistive model with a single NTM island is consistent with the evolution inside the island location. During the quasi-steady conditions a single NTM is not sufficiently strong to explain the flattening of the q -profile near the magnetic axis. In other simulations with an additional NTM resonant closer to the magnetic axis, e.g. a (4,3) mode, we were not able to obtain the flat q evolution; this needs to be explored in greater detail. Thus, in the region near the magnetic axis, we couple to the WJ hyper-resistive model [8] that also conserves helicity and adds to the effect of the BFLP model but over a different spatial region, Fig. 6. WJ gives a transient correction to the q -profile near the magnetic axis with the negative sheet current forming as a direct consequence of the hyper-resistive model conserving helicity. The current and q then relax as the current re-peaks due to a combination of normal flux diffusion and current diffusion in the vicinity of the island. The form of the WJ hyper-resistivity requires the presence of a $q=1$ surface (e.g. (1,1)-like mode). It diffuses the current so as to alter the poloidal and toroidal flux distribution inside the $q=1$ radius and tends to flatten the current and q -profiles. As we show in Fig. 6, the NTM mode is still active in the mid-radius region and continues to modify flux diffusion in the core region inside the island location. The BFLP interaction thus limits the radial extent of the WJ-induced current diffusion. This coupling comes in dynamically through the equilibrium evolution that is solved at each

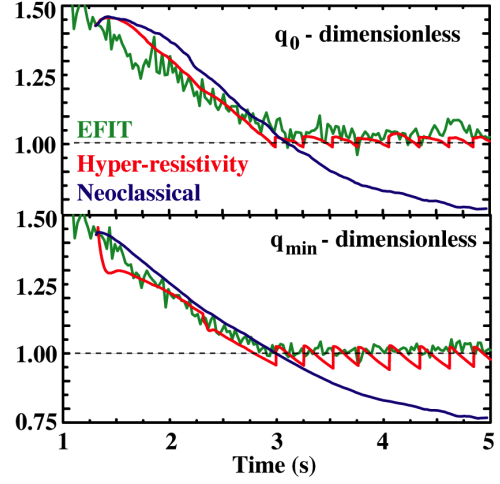


FIG. 4. Consistency of q_0 and q_{\min} evolution between HR-simulations and MSE-constrained EFIT and the comparison with neoclassical. The q -profile responds to the change in mode from (5,3) to (3,2) at 2,3 s. The quasi-constant q is due to a combination of WJ limited by BFLP and flux diffusion rebuilding the current at the axis.

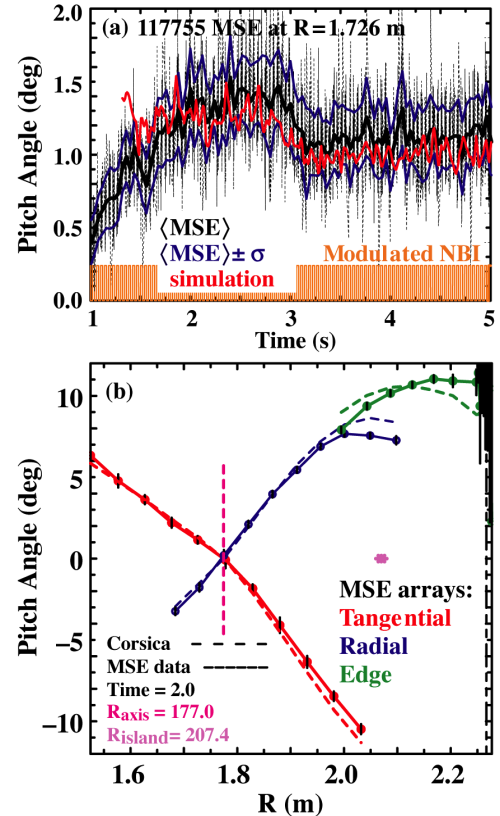


FIG. 5. MSE pitch angles (B_p/B_t): (a) measured data (grey), $\langle \text{MSE} \rangle$ averaged over the beam-on time, $\langle \text{MSE} \rangle \pm$ one standard deviation and the simulated MSE data near the magnetic axis and (b) comparison of simulated and measured MSE data at $t=2s$.

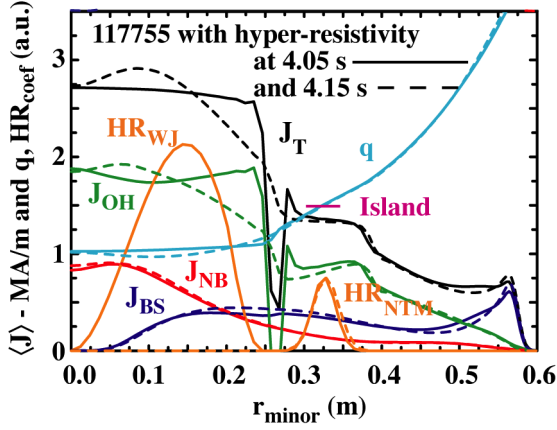


FIG. 6. Flux-averaged current densities $\langle J \rangle$, q , and normalized HR 4.05s (solid) showing current diffusion due to the WJ HR flattening of the q profile near the axis. The radial extent is limited by the presence of BFLP HR modifying the current and flux evolution in the island region. Also shown is a rebuilding of current (dotted) due to flux and current diffusion that causes q_{\min} to decrease with time.

core have been obtained in the JET [19], JT-60U [20] and ASDEX-Upgrade [21] tokamaks. In DIII-D experiments, current holes [22] having a maximum width of 0.5 m ($\sim 45\%$ of the plasma diameter) at the mid-plane have been obtained with somewhat narrower current holes sustained for 1.1 to 2.5 s in discharges lasting up to 6 s. These durations are near the current relaxation time and 10-20 energy confinement times. Core temperatures for ion up to 22 keV and electron up to 4 keV were obtained with up to 6 MW of neutral beam power and 2.5 MW of ECH power and a line-averaged density of $\sim 2 \times 10^{19} \text{ m}^{-3}$. The deep negative central shear in “Current Hole” (CH) plasmas is highly conducive to the formation of such ITBs. Such discharges are produced with a fast plasma current ramp and hot core plasma that slows inward flux diffusion while the back EMF due to non-inductive current drive further cancels any plasma current in the core. Such CH plasmas have zero or near zero poloidal field in the core and thus temperature and particle density gradients are negligible due to the lack of good confinement. At the edge of the current hole, the poloidal field rises sharply and the resulting improved confinement yields sharp temperature, density and pressure gradients. The sharp density and temperature gradients gives rise to a significant bootstrap current and indeed the establishment of these gradients appears to widen the current hole as is seen in present discharges.

Since the shear is strongly negative in the core, it is expected that fast-ion instabilities such as Alfvén modes, e.g., cascade modes, would occur in the core region. These, in turn, are expected to cause fast-ion redistribution and loss [23] and this can also add to the steepness of pressure gradients at the edge of the current hole. Therefore, the evolution of a CH plasma appears to be a self organizing phenomenon with self-consistent current, temperature and density profiles sustaining a current hole. In order to investigate the fast-ion behavior, the consistency between the pressure profile (which includes calculated fast-ion pressure) and the neutron flux is examined for different models of fast-ion diffusion in the plasma.

We carried out careful equilibrium reconstructions making use of both MSE and magnetic probe data and fit constraints optimized to give best convergence and fit to the data. We

time step in the simulation. Even though the WJ model relies on a $q=1$ resonance, q_0 and q_{\min} in the quasi-stationary interval, Fig. 4 at $t > 3$ s, is consistent with the EFIT solutions and both exhibit weak negative shear near the magnetic axis. The simulated q_{\min} tends to drop further below 1 due to details of the current density profile modeling in the core, where the non-inductive components, J_{BS} and J_{NB} are comparable to the J_{OH} due to flux diffusion effects as the current density rebuilds. As previously noted, the quasi-stationary temporal evolution of the simulated and measured MSE data, Fig. 5(a), near the magnetic axis indicate a statistical consistency in this region.

4. Current Hole Evolution

In typical tokamak plasmas the current density is peaked on axis. Converse examples of discharges with very hollow or zero current in the

obtained kinetic equilibrium fits using the TRANSP code with Fig. 7 (*) showing the pressure profile resulting when a uniformly large fast-ion diffusion coefficient across the plasma is used. While this pressure profile is consistent with the observed neutron flux, it leads to a poorly converged equilibrium with negative core currents. In order to obtain agreement between measured and calculated neutron flux and also obtain a converged equilibrium, we need to use a very high value for the anomalous fast-ion diffusion in the core. This results in a pressure profile that is similar to that predicted by equilibria obtained using only magnetic probe and MSE data. In Fig. 7 we show (+) the calculated pressure profile that corresponds to the maximum core pressure that does not give a negative current in the core. For comparison, we also show results with a uniform fast-ion diffusion coefficient of $7500 \text{ m}^2/\text{s}$. It may also be noted that only the MSE EFIT (solid) agrees well with the final equilibrium fit (dashed).

In Fig. 8, we show the components of the parallel current density for the CH equilibrium of 119817 case B, calculated by TRANSP. The bootstrap current (NCLASS) calculated inside the current hole by “neoclassical” packages in codes such as TRANSP is not valid [24] and the dotted line is an extrapolation to illustrate the likely current profile according to the reference. The TRANSP-calculated neutral-beam-driven current is also expected to be much smaller than that shown. The difference between the total parallel current and the sum of the two non-inductive currents shown is the Ohmic (inductively driven) current. It is evident from this plot that the all currents are self-organized by the plasma to get a current hole where: (1) the negative central shear creates a transport barrier that results in a bootstrap current at the edge of the current hole and causing a sharp current gradient, (2) the lack of poloidal flux in the core and the resulting poor confinement sets all gradients to be small thereby making for near-zero bootstrap current inside the barrier, and (3) TRANSP-based equilibrium is consistent with strong fast-ion redistribution that in-turn causes the neutral beam current drive in the core to be small and also keeps the pressure gradient low in the core.

5. Summary

In summary, we present analyses and modeling for two distinct modes of operation on DIII-D that appear to require anomalous current diffusion and/or self-organization: hybrid modes generated from H-mode-like conditions and high confinement hollow-current profile discharges. Using hyper-resistive current diffusion models that coupling different

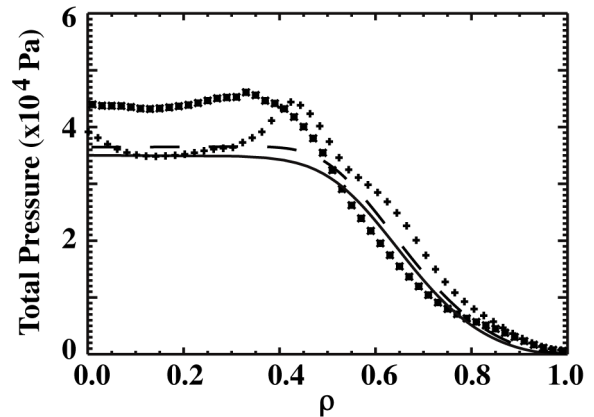


FIG. 7. Pressure profiles: (*) TRANSP with uniform fast-ion diffusion, (+) maximum for non-negative core current, (—) from MSE EFIT, and (---) final equilibrium.

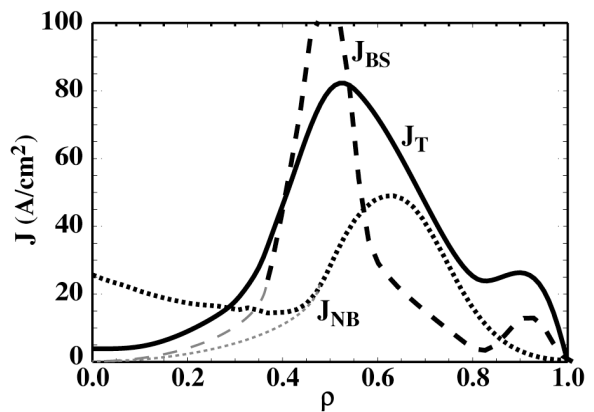


FIG. 8. Parallel current density components for the current hole equilibrium. The “grey” regions of J_{NB} and J_{BS} approaching 0 at the axis are required currents consistent with J_T from the best-fit equilibrium.

regions through the equilibrium, we demonstrate that anomalous current evolution effects are capable of explaining the hybrid-mode current-density profile evolution and the finally achieved quasi-stationary conditions. Current diffusion from the BFLP model in the vicinity of an NTM island continuously adjusts the evolving q -profile near the mid-radius region. During the steady conditions, the NTM island continues to adjust the q -profile while limiting the radial extent over which the WJ model adjust q near the magnetic axis. The magnetic pitch angles from a synthetic MSE diagnostic used in the simulations are consistent with the MSE measurements. In the case of the current-hole formation, the fast-ion instabilities resulting from the negative shear configuration result in enhanced diffusion of beam-injected ions that in turn reduces the neutral-beam current drive near the magnetic axis. The creation of an internal transport barrier due to the negative shear maintains global confinement and results in the peaking of the current density at the barrier edge where steep gradients form. This self-organization mechanism, e.g., negative shear giving rise to both instabilities and a barrier, generates conditions favorable for sustaining the current-hole plasma configuration. Modeling of these effects are consistent with equilibria produce by MSE-constraint fitting to the experiment.

Work supported by the U.S. Department of Energy under DE-FC02-04ER54698, DE-FG02-95ER54309, W-7405-ENG-48, DE-FG03-97ER54415, DE-AC05-00OR22725, and DE-AC02-76CH03073.

References

- [1] LUCE, T.C., et al., Nucl. Fusion **41** (2001) 1585.
- [2] STAEBLER, A., et al., Nucl. Fusion **45** (2005) 617.
- [3] GREENFIELD, C.M., et al., Phys. Rev. Lett. **86** (2001) 4544.
- [4] CHU, M.S., "Maintaining the Quasi-Steady State Central Current Density Profile in Hybrid Discharges", this meeting, paper EX/1-5.
- [5] CROTINGER, J.A., et al., Lawrence Livermore National Lab. Report UCRL-ID-126284, 1997 available from NTIS #PB2005-102154.
- [6] BOOZER, A.H., J. Plasma Phys. **35** (1986) 133.
- [7] BERK, H., et al., UCRL-ID-142741 (2001) from <http://www.osti.gov/bridge>
- [8] WARD, D.J., and JARDIN, S.C., Nucl. Fusion **29** (1989) 905.
- [9] RECHESTER, A.B., and ROSENBLUTH, M.N., Phys. Rev. Lett. **40** (1978) 38.
- [10] HEGNA, C.C., Phys. Plasmas **5** (1998) 1767.
- [11] La HAYE, R.J, Phys. Plasmas **13** (2006) 055501.
- [12] KOTSCHENREUTHER, M., et al., Phys. Fluids **28** (1985) 294.
- [13] CASPER, T.A., et al., "Study of Current Profile Evolution in Presence of Tearing Modes in DIII-D Hybrid Discharges", Plasma Phys. 2004 (Proc. 31st EPS Conf. London, 2004) ECA 28G, P2.178.
- [14] HOULBERG, W.A., et al., Phys. Plasmas **4** (1997) 3230.
- [15] PEARLSTEIN, et al., Plasma Physics (Proc. 33rd EPS Conf. Rome, 2006) P5.128.
- [16] HOLCOMB, C.T., et al., Rev. Sci. Instrum. **77** (2006) 1.
- [17] CASPER, T.A., et al., Rev. Sci. Instrum. **75** (2004) 4193.
- [18] THOMAS, D.M., et al., Phys. Plasmas **12** (2005) 056123.
- [19] HAWKES, N.C., et al., Phys. Rev. Lett. **87**(11) (2001) 115001.
- [20] FUJITA, T., et al., Phys. Rev Lett. **87**(4) (2001) 245001.
- [21] MERKL, D., et al., Contr. Fusion and Plasma Phys. (Proc. 30th EPS Conf. St. Petersburg, 2003), ECA vol. 27A, p. P-1.134.
- [22] JAYAKUMAR, R., Nucl. Fusion, to be submitted.
- [23] YAVORSKIJ, V., et al., Nucl. Fusion **43** (2003) 1077.
- [24] BERGMANN, A., Phys. Plasmas **8**(12) (2001) 5192.